Available Online at http://www.journalajst.com

ASIAN JOURNAL OF SCIENCE AND TECHNOLOGY

ISSN: 0976-3376

Asian Journal of Science and Technology
Vol.06, Issue, 12, pp.2139-2150, December, 2015

RESEARCH ARTICLE

ZINC OXIDE NANOPARTICLES IMPREGNATED POLYMER HYBRIDS FOR EFFICIENT EXTRACTION OF HEAVY METALS FROM POLLUTED AQUEOUS SOLUTION

Beaulah Angelin, K., Siva, S. and *Sayee Kannan, R.

Department of Chemistry, Thiagarajar College, Madurai-625009, India

ARTICLE INFO

Article History:
Received 12th September, 2015
Received in revised form
25th October, 2015
Accepted 07th November, 2015
Published online 30th December, 2015

Key words:

FT-IR,
n-ZnO composite,
Thermodynamics,
Adsorption,
Kinetics.

ABSTRACT

The aim of this research work is to investigate the exploitation of the nano zinc oxide composite was used as an adsorbent for the removal of Pb(II), Hg(II), Cd(II) and Bi(III) heavy metal ions from aqueous solution. The resulting adsorbent n-ZPFR was characterized by SEM with EDS, BET, TEM, FT-IR, XRD, DTA and TGA analyses and tested for metal adsorption. The maximum adsorption performance was achieved for Pb(II), Hg(II), Cd(II) and Bi(III) ions from aqueous solution by n-ZPFR was investigated as a function of some parameters such as initial metal ion concentration (0.01M), contact time (60min), dose (0.250g) and temperature (328K). Langmuir, Freundlich, Dubinin Kaganer-Radushkevich, Temkin and Jovanoic isotherm models were used to interpret the experimental data. The data obeyed both D-R and Jovanoic models (R2=0.999) indicating a monolayer adsorption of heavy metal ions onto the homogeneous surface. The linear plot of Temkin isotherm showed adsorbent adsorbate interactions. Moreover, the energy obtained from D-R isotherm (2579.8-426.9 KJ/mol) indicated a physical adsorption of the metal ions onto the adsorbent surface. Kinetic studies indicated that Pb(II),Hg(II),Cd(II) and Bi(III) ions adsorption followed the pseudo-second-order model. Kinetics; controlled by both liquid-film and intra-particle diffusion mechanisms. The thermodynamics parameters (ΔG0, ΔH0 and ΔS0) of adsorption systems indicated spontaneous and endothermic process. The results suggested that n-ZPFR composite is economical, eco-friendly and capable to remove Pb(II), Hg(II), Cd(II) and Bi(III) from natural water resources.

INTRODUCTION

Environmental Pollution today has far-reaching negative consequences on human lives. Water pollution is increasing worldwide due to rapid growth of industry, increase the human population, domestic and agricultural activities which leads to the life time threatening diseases (Schwarzenbach *et al*., 2010). Degradation of organic pollutants that have deleterious effects on human well-being has become a focus of current scientific research effort. Heavy metal ions are dangerous constituents of waste waters because of their toxicity to living systems even at low concentrations (Fujita *et al*., 2014). The pollution of the environment with heavy metals is a result of human activities, and the effects of these toxic metals on the ecosystems are of public health significance. Toxic metals can be distinguished from other pollutants, since they are not biodegradable and can be accumulated in living tissues, causing various diseases and disorders. The increasing levels of toxic heavy metal ions discharged into the environment have received considerable attention due to the adverse effects on receiving waters.

Corresponding author: Sayee Kannan, R.,
Department of Chemistry, Thiagarajar College, Madurai-625009, India.

These include metal ions such as lead (Pb), Chromium (Cr), Copper (Cu),Cadmium (Cd), Nickel (Ni), Silver (Ag), Mercury (Hg) and Zinc(Zn).The potential sources of heavy metal ions in wastewaters include fertilizers, fungicides, metals used in manufacturing paints, pigments and batteries. Although few natural sources are concerned for lead existence such as soil-erosion, volcanic emissions, mining,but industrial activities delivered about 90% of lead into environment, where lead-containing dust particles are significantly polluted the air as well as soils. (Inglezakis *et al*., 2003; Barakat, 2011). Because of their high solubility in the aquatic environments, heavy metals can be absorbed by living organisms. Once they enter the food chain, large concentrations of heavy metals may accumulate in the human body. The accumulation of lead in the human body causes chronic poisoning which include mental retardation to infants and kidney problem to adults (Kawasaki *et al*., 2006). Mercury has very tendency of binding with proteins and it mainly affects the renal and nervous systems. This metal ion is a hazard to public health and the environment when discharged inappropriately. (Denizli *et al*., 2003) In recent years the new promises that nanotechnology offers have spurred the industry to focus their research and investments on developing new applications such as purification of air, water and hazardous waste. In order to detoxify heavy metals various techniques have been employed.

Among these nano-based adsorbents are the more effective technologies for the removal of heavy metal ions from the aqueous system. Application of zinc oxide based nano material composite polymer-resin are more effective for removal of heavy metals contamination from the water because of their important features like high surface area, small size etc. So Nanoparticulates have much larger surface areas than bulk materials and exhibit novel properties due to their small size (Dlarmendra *et al*., 2008).

In recent years,variety of nanomaterials such as carbon nanotu bes (Mohamed Abdel Salam and Robert C.Burk, 2010), TiO_2, (Senthilnathan and Ligy Philip, 2010), magnetic chitosan Nanocomposite (Xiaowang Liu *et al*., 2009), magnetic Fe_3O_4 (Jing-Fu Liu *et al*., 2007), surface modified $MnFe_2O_4$ (Jing Hu *et al*., 2005), alumina (Rahmani *et al*., 2010) etc., have been investigated for their tendency towards the removal of toxic metals. Nanosized zinc oxides as an environmental friendly material, ZnO can be used in catalyst industry, gas sensors, solar cells and so on. As an adsorbent ZnO was mostly applied to eliminate H_2S. Recently, people have found that nanostructured ZnO could efficiently remove heavy metals. Thus, the main objectives of this paper are; i) To determine the physic-chemical characteristics of nanocomposities, ii) To identify the various parameters like pH, initial concentration, contact time and temperature on adsorption capacity of ZnO have been investigated. The adsorption potential of synthesized ZnO nanoparticles in the removal of Pb(II), Hg(II), Cd(II) and Bi(III) ions from aqueous solutions has been studied. Based on these adsorption studies, to analyze the equilibrium uptake capacity of the adsorption process from various adsorption isotherms models like Langmuir, Jovanoic isotherm equation. Finally the adsorption kinetics and thermodynamics of these ions were evaluated.

MATERIALS AND METHODS

Materials

The chemicals used in the present study were Conc. Sulfuric acid (Specific gravity = 1.82), Formaldehyde (37-40% solution) and Phenol (Density=1.057gm-1), Zinc Oxide (30 nm, molecular weight,81.38) was supplied by SRL chemicals, Mumbai, India. The Mercury(II) Chloride ($HgCl_2$,M.W.271.50) and lead Nitrate ($Pb(NO_3)_2$,M.W.331.21), Cadmium Nitrate tetra hydrate ($Cd(NO_3)_2.4H_2O$M.W.308.47), Bismuth(III) Nitrate pentahydrate ($Bi(NO_3)_3.5H_2O$M.W.485.07) was obtained from RANKEM chemicals New Delhi, India. All the chemicals used were analytical grade. The double distilled (DD) water was used throughout the investigation.

Preparation of nano ZPFR composites

Phenol and Conc. Sulfuric acid (1:1) and 0.5 mg of nano Zinc oxide were mixed slowly with constant stirring in an ice bath. The mixture was then, heated to 70°C for six hours, cooled and kept overnight. The product was polymerized with formaldehyde solution (12.5 ml) in an ice bath, and then heated to 80°C for three hours and the product was cured, then ground washed with DD water, to remove the free acid. Then the sample was dried at 70°C for 16 h. Then the composite resin were sieved and preserved for characterization and further studies (Kannan and Seenivasan, 2007).

Adsorption experiments

Batch adsorption experiments were carried out by adding certain amount of adsorbent in a set of 250ml conical flasks containing 40ml of metal ion solutions with various initial concentrations, dose, contact time and temperatures in a thermo stated water bath shaker and shaking speed of 200rpm for 1hr. After above treatments the samples were centrifuged to separate the solutions from the adsorbent at 4000rpm for 5mts. Then 1ml of the supernatants was diluted to a suitable concentration and the absorbance of the supernatants solution was measured before and after treatment using atomic absorption (Elico SL-173) spectrometry at wavelength of 283.3,253.7,458,253nm for Pb(II), Hg(II),Cd(II) andBi(III). Each experiments was carried out in twice under identical conditions and an average value was employed. The P^H of the metal ion solution was adjusted by using NaOH or HCl solution and a P^H meter. The different temperature was carried out in adsorption studies. This thermodynamic parameter was used to determine the effect of temperature in adsorption studies. The adsorption efficiency and amount of adsorption in batch experiments were calculated as follows:

$$\mathbf{q = (C_o - C_e)\, V / m} \quad \text{…… (1)}$$

$$\mathbf{Efficiency\ (\%) = (C_o - C_e) / C_o \times 100} \quad \text{…….. (2)}$$

Where, C_o is the initial concentration (mg/L)
C_e is the equilibrium concentration (mg/L)
V is the volume of solution (mL)
m is the mass of adsorbent (g)
q is the amount of adsorbed (mg/g)

Desorption experiments

The desorption studies of the adsorbed metal ions from ZnO nanocomposities were carried out by HCl eluent solutions of different concentration and stirred at 200rpm for 12h at room temperature. For regeneration the adsorbent was removed from the solution and rinsed with DD water. The adsorption-desorption cycles were repeated for 3 times to establish the reusability of the adsorbent, the desorption percentage (E) was calculated as follows:

$$\mathbf{E\ (\%) = C_d V_d / (C_o - C_e) \times 100} \quad \text{…….. (3)}$$

Where, E is the desorption ratio,

C_d is the concentration of the solutes in the desorption solutions,
V_d is the volume of the desorption solution and
C_o, C_e and V are the same as defined above

RESULTS AND DISCUSSION

Effect of adsorbent activity

The sorption of Pb, Hg, Cd, and Bi by ZnO nanomaterials was studied. ZnO nanomaterials have good sorption capacities for toxic heavy metals.

The activity of adsorbent for the adsorption of Pb (II),Hg (II), Cd(II) and Bi(III) was studied with an initial concentration of 0.01M,adsorbent dose of 0.250 g and contact time of 60 min and the results were shown in (Fig.1) the order of adsorption activity for the removal of all the metal ions was n-ZPFR > PFR > n-ZnO.n-ZPFR composite resin exhibited higher adsorption activity (97.1% ,86.8%,80.9% and 61.2%) than compare to other resin . n-ZPFR composite resin had high removal efficiency than PFR and n-ZnO due to more exposed active sites resulted in high removal of metal ion adsorption and high surface area.

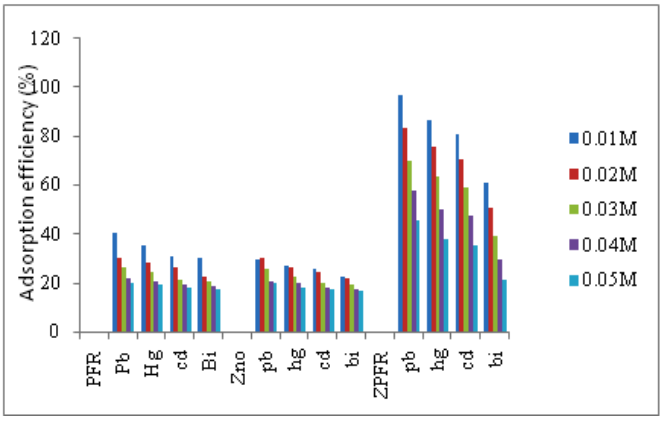

Figure 1. Adsorption activity of PFR, n-ZnO, and n-ZPFR

Characterization of the adsorbent

B.E.T: Specific surface area and pore volume analysis

The surface area was calculated by the Brunauer- Emmert-Teller (BET) equation. The BET specific surface area was measured on the thermal analysi s instrument through the adsorption of Nitrogen. The surface area of n-ZPFR was 26.4111 m²/g with R^2=0.999. The average pore radius of n-ZPFR was 10.90 Å and total pore volume was 0.11962 cm³/g. As shown in (Fig.2) the isotherm could be classified as IV type isotherm which is characteristics of the mesoporous materials (Chang *et al*., 2012).

The porosity and the specific surface area of n-ZPFR nano co mposites were investigated through the nitrogen adsorption/de sorption isotherms.The relative adsorption performance of different adsorbent is highly dependent on the internal pore structure of each material. With the increase of pore radius, more adsorbate is easier to be adsorbed. It is not only able to increase the surface area and average pore radius but also reinforce the chemical strength of adsorbents in acidic medium. It is interesting to note that n-ZPFR composites showed higher surface area compared to other nanocomposites (Zhao *et al*., 2011; Zhang *et al*., 2013; Oh *et al*., 2013; Liu *et al*., 2013; Cheng *et al*., 2012). Therefore, carbon activation offered some attractive advantages.

FTIR

The FT-IR technique was used to monitor changes on the surface of the ordered mesoporous carbon. The FT-IR spectra were performed in the range of 400 – 4000cm^{-1} .The infrared spectra of the nanoparticles were taken in KBr pressed pellets on a NEXUS670 infra fourier transform spectrometer Nico-let Thermo, Waltham. MAI.

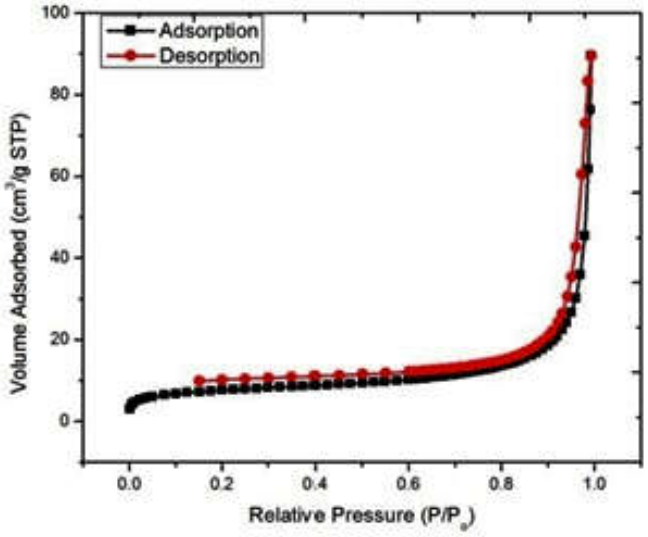

Figure 2. Adsorption-desorption isotherms of nitrogen at 77 K on n-ZPFR

The spectra of the n-ZnO, n-ZPFR, n-ZPFR-Pb(II),n-ZPFR-Hg(II).n-ZPFR-Cd(II) and n-ZPFR-Bi(III) were shown in (Fig.3). In (Fig.3a). The FT-IR spectra of pure n-ZnO displays sharp peak absorption band observed at 1383.9cm^{-1} corresponding to stretching vibration. Moreover the broad peaks obtained between 3434.0cm^{-1} are due vibration mode of intermolecular H bonds present in sample.(Fig.3b) showed the FTIR spectrum of n-ZPFR the broad peak at 3412.0 cm-1 indicated the presence of OH groups on the surface of n-ZPFR.

The two characteristic bands at 1642.1 cm-^{1} and 1029.7 cm-^{1} due to the corresponding C=C and C-O-C stretching vibrations. The another two bands occurred at 1469.8 and 882.2 cm-^{1} were observed due to the presence of C=C and C-H stretching in the aromatic ring.(Fig.3c) FTIR data of n-ZPFR-Pb showed that characteristic band at 3436.3, 1645.4, 1464.8 and 1207.2 cm-1 correspond to the OH groups, C=C stretching, C-H bending vibrations and C-O-C stretching vibrations. The sharp peak at 1032.4 cm^{-1} corresponds to the C-O stretching vibrations were involved in Pb(II) ion adsorption respectively. (Fig.3d). FTIR data of n-ZPFR-Hg(II) showed that characteristic bands at 3394.2, 2923.2, 1642.6 and 1033.4 cm-1 corresponding to OH, =C-H, C=O,C=C stretching vibrations respectively whereas one sharp peak observed at 1471.0cm^{-1} corresponding to C-H bending vibrations were involved in Hg(II) ion adsorption. (Fig:3e) FT-IR data of n-
ZPFR Cd showed that characteristic band at 3429.6,1465.8,10 35.8 cm^{-1} correspond to the OH groups, C-H bending vibration, C=C stretching vibrations.

There was a sharp band at 1645.4cm^{-1} which was the feature of the presence of C=O stretching vibrations were involved in Cd(II) ion adsorption.(Fig.3f) FT-IR data of n-ZPFR-Bi(III) observed the broad peak at 3435.9cm^{-1}were attributed the presence of intermolecular H bonds. FT-IR data of n-ZPFR-Bi(III) showed that characteristic band at 1644.9,1464.5,1032.7cm^{-1} correspond to the C=O stretching

vibrations, C-H bending vibrations and C=C stretching vibrations were involved in Bi(III) ion adsorption respectively (Zagorodni *et al*., 2002).

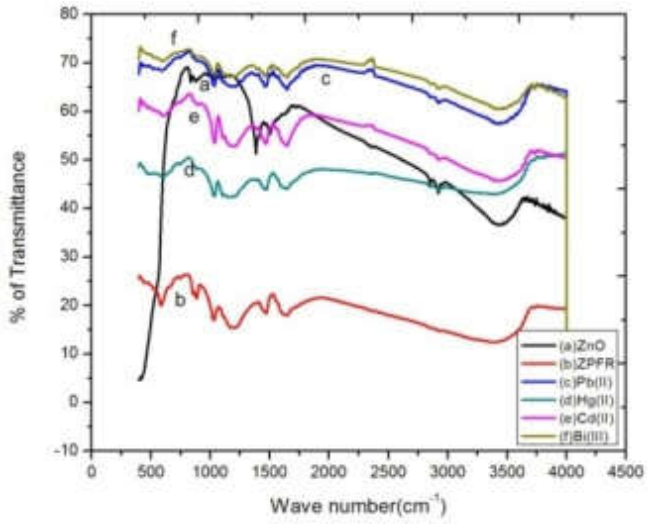

Figure 3.FTIR spectra of;(a) n-ZnO (b) n-ZPFR (c) n-ZPFR-Pb(II) (d) n-ZPFR-Hg(II) (e) n-ZPFR-Cd(II) (f) n-ZPFR-Bi(III)

XRD

In order to confirm the crystalline nature of ZnO nanoparticles on n-ZPFR composite, XRD pattern has been studied. The characteristic 10˚-60˚ peaks of n-ZPFR were discernible in carbon, the diffraction spectrum of n-ZPFR Pb(II) shows crystalline peak at the scan range 20-50˚ thereby indicating the crystalline phase of n-ZPFR. The XRD pattern was collected in the 2 theta range from 10^0 to 80^0. In (Fig 4a) shows the no peaks of any other phases are detected from the XRD pattern, which are attributed to the n-ZPFR showed amorphous carbon.In (Fig.4b) shows the XRD pattern of n-ZPFR-Pb(II) the characteristic diffraction peaks at 2ɵ = 20.8^o , 24.5^o ,26.6^o, 29.6^o , 33.1^o , 43.7^o represent the corresponding indices (120) (002) (030) (221) (310) (400), respectively (Nata *et al*., 2010; Zhang *et al*., 2011). The peak positions and relative intensities of the n-ZPFR composite are in good agreement with those from the JCPDS card no PDF ≠ 231496, which reveals the well-known ortho rhombic structure of Zn_2PbO_4.The average crystalline size of n-ZPFR was 8nm.

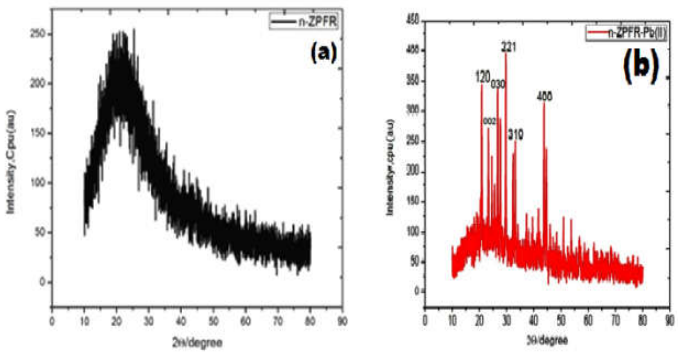

Figure 4. XRD pattern of free (a) and Pb (II) loaded (b) n-ZPFR

SEM

SEM (Scanning Electron Microscopy) studies provide useful information regarding the surface morphology of the materials which their records are shown in (Fig.5a) the SEMs of n-ZPFR, n-ZPFR-Pb(II), n-ZPFR-Hg(II), n-ZPFR-Cd(II) and n-ZPFR-Bi(III) ions. As can be seen the synthesized ZPFR had an approximate spherical shape with a mean diameter of about 1µm.This images illustrate that the ZnO nanoparticles have holes and some small openings on the surface, which increases the contact area and can improve metal ion adsorption.

(Fig.5b,5c 5d and 5e) showed micrographs of the n-ZPFR surface after adsorbed Pb (II) ions, Hg (II) ions, Cd(II) and Bi(III) the surface of n-ZPFR was relatively smoother and less porous because of the formation of a layer over the adsorbent surface after adsorption of metal ions. Decreasing size of the nanoparticles with mole fraction of dopant ions can be attributed to internal strain of the lattice (24) (Sankar *et al*; 2013).

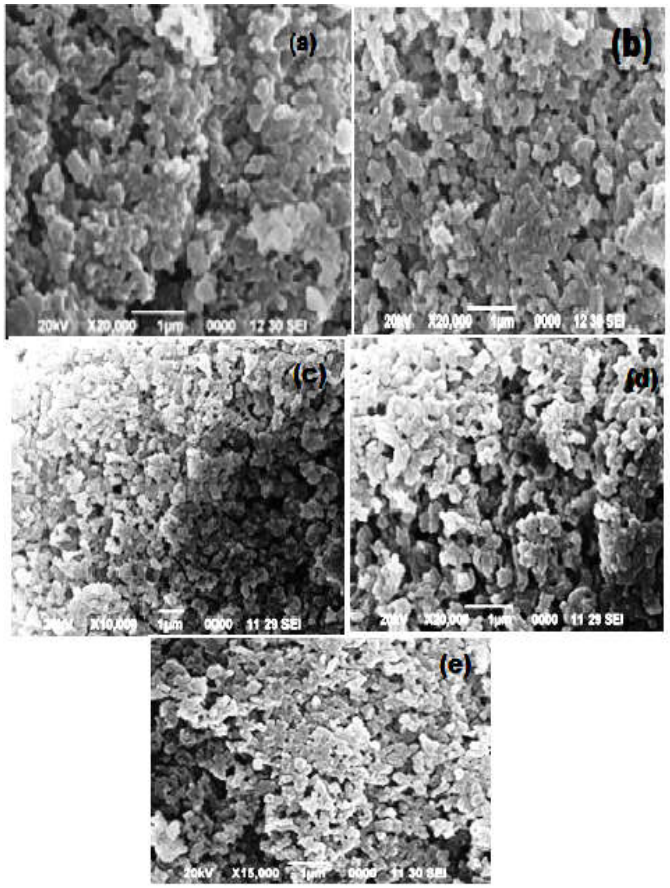

Figure 5. SEM images of (a) n-ZPFR (b) n- ZPFR-Pb (II) (c) n-ZPFR-Hg (II) d) n- ZPFR-Cd (II) e) n- ZPFR- Bi (III).

EDX

Further confirmation of the adsorption of Pb(II),Hg(II),Cd(II) and Bi(III) on n-ZPFR composite was done by energy dispersive X-ray analysis (EDS). (Fig.6a) for the unloaded n-ZPFR, did not show any characteristic signal for metal ions, but only showed for the four major constituents, i.e., C, O, Zn and S. Whereas for Pb (II), Hg(II), Cd(II) and Bi(III) loaded (Fig.6b 6c 6d and 6e) signals of presence of Pb(II), Hg(II), Cd(II) and Bi(III) were observed. This showed the diffusion or accumulation of metal ions onto the surface of n-ZPFR (25) (Kannan *et al*; 2011).

TGA/DTA Analysis

The TGA thermo grams for the n-ZPFR samples were shown in (Fig.7a). The thermo gravimetric profile revealed that the mass loss occurs in three stages (26).

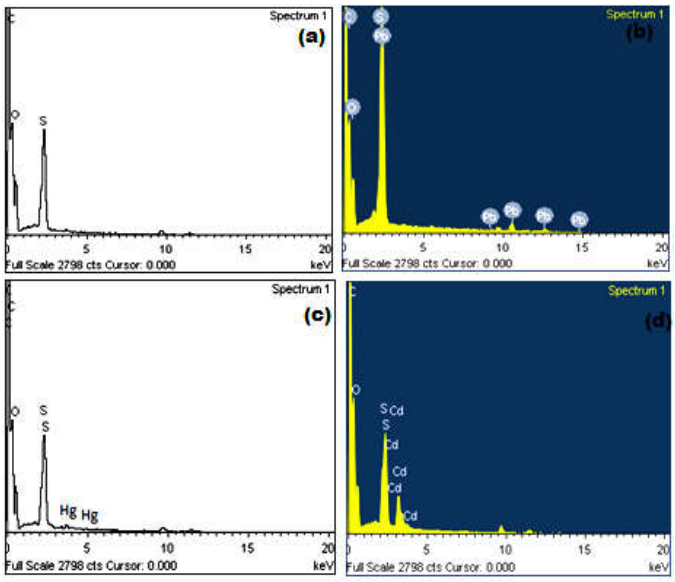

Figure 6. Energy dispersive spectra of a) n-ZPFR b) n-ZPFR-Pb(II) c) n-ZPFR-Hg(II) d) n- ZPFR-Cd(II)

The first weight loss about 95.4% in that temperature range 100-110°C, which may be the combined water existed in n-ZPFR composite. The second weight loss occurred in the temperature range 300-350°C, a typically high enough temperature to induce thermal degradation of ordinary carbon polymers which about 75.6%. The final weight loss was determined above 600-700°C, which about 56.9%. Finally, no mass loss was detected when the temperature was increased to 750ºC. This result indicated that the n-ZPFR are stable at higher temperature. The char residue of n-ZPFR content was 33.6%.The characterization results confirmed that the formation of the adsorbent n-ZPFR occurred successfully.In (Fig.7b) shows the loss of water and n-ZPFR composite was evidenced by endothermic peak was obtained.Two sharp peak indicates the chemical changes occurring due to thermal degradation of the n-ZPFR composite.At 560^{o}c , the presence of one broad peak indicate the dehydration of n-ZPFR (27) (Thongnopkum *et al*., 2012).

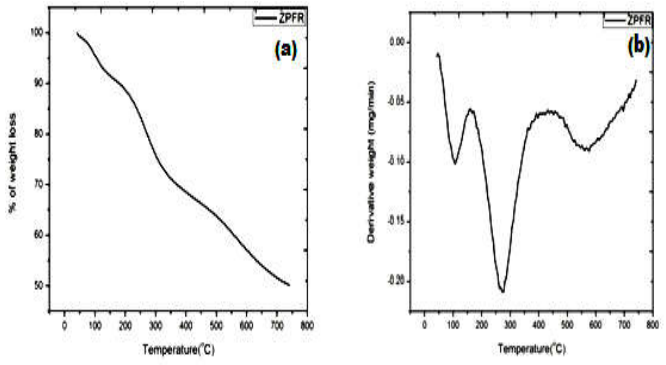

Figure 7. TGA (a) and DTA curve (b) of n-ZPFR

TEM

The morphology and size of nanoparticles were studied by transmission electron microscopy (TEM). The image revealed that the particle size of the composite was 10nm (Fig.8a and Fig8b).

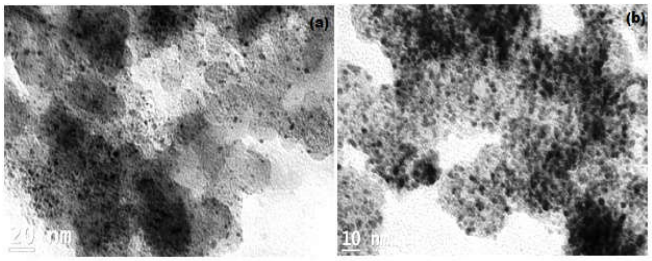

Figure.8 TEM images of free (a) and Pb (II) loaded n-ZPFR.

Electron diffraction analysis

The electron diffraction patterns of ZnO nanoparticles and n-ZPFR composite (Fig.9a and Fig 9b) were studied. The fringe ring pattern clearly indicated the amorphous nature of the zinc oxide nanoparticles. The fused ring pattern revealed the crystalline nature of the n-ZPFR composite.

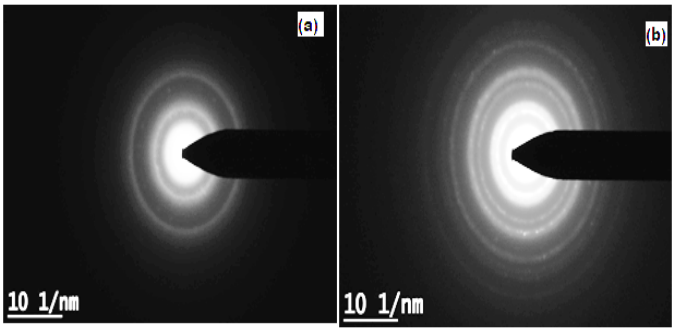

Figure 9. Electron diffraction of a) n-ZPFR b) n-ZPFR-Pb(II)

Effect of initial concentrations of heavy metal ions

The adsorption capacity is dependent on the initial metal ion concentration. The dependence of adsorption capacity of ZnO nanoparticles was studied at different initial metal ion concentrations in the range of 20-60 mg/L at 298 K with 0.250 g n-ZPFR at 60 min. The percentage of Pb (II), Hg (II), Cd(II) and Bi(III)ions adsorption at different metal concentrations using n-ZPFR, decreased with increase in metal ion concentration. This may be due to saturation of active adsorption sites onto n-ZPFR. The effect of initial concentration on the removal of Pb (II), Hg (II), Cd(II) and Bi(III) by the adsorbent was indicated in (Fig.10) (28)

Effect of contact time on adsorption

The effect of contact time on metal ion adsorption is shown in (Fig.11). The adsorption capacity of Pb(II), Hg(II), Cd(II) and Bi(III) adsorption increased with increasing the contact time, the maximum removal of all the metal ions occurred at 60 min, after which there were no significant changes. Hence in the present study 60min was chosen as the equilibrium time.

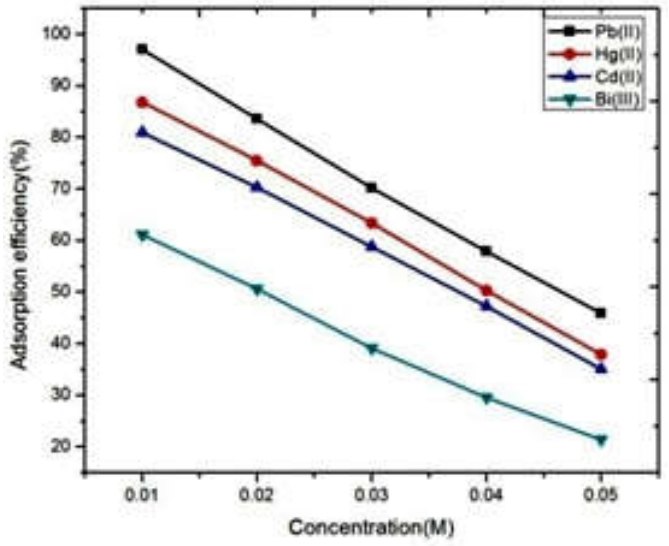

Figure.10.Effect of initial concentration on the removal of Pb(II), Hg(II), Cd(II) and Bi(III) from aqueous solution

The adsorption rate was fast and the maximum adsorption was achieved almost within 60min for all the metal ions. Because of the availability of more active sites and more functional groups which participate in the metal ions uptake till equilibrium is attained and thereafter, there was no further adsorption. The contact time is one of the important parameter s for economical wastewater treatment application. (Smiciklas *et al*., 2008).

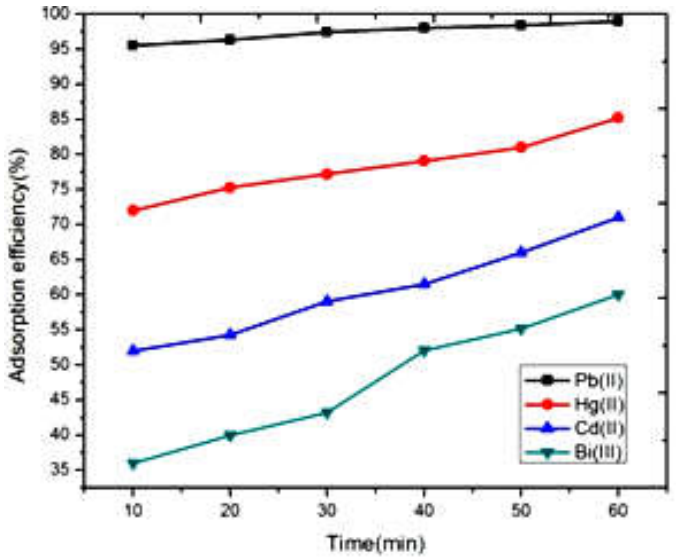

Figure.11. Effect of contact time on the removal of Pb(II), Hg(II), Cd(II) and Bi(III) from aqueous solution.

Effect of adsorbent mass

The effect of adsorbent dosage on Pb(II), Hg(II), Cd(II) and Bi(III) removal was studied by varying the amount n-ZPFR between 0.050-0.250g. The increased metal ion removal percentage at increasing adsorbent dosage is due to increased active sites and surface area for adsorption at higher adsorbent dosage. That is, the percentage removal increased from 45.9% to 97.1% for lead, mercury was increased from 37.9% to 86.8%, Cadmium increased from 35.1% to 80.9% and Bismuth increased from 21.4% to 61.2% as the n-ZPFR adsorbent were shown in (Fig:12).The optimum adsorbent dosage was found to be 0.250 g for Pb(II),Hg(II),Cd(II) and Bi(III). The adsorption efficiency of Pb(II),Hg(II),Cd(II) and Bi(III) was observed at 97.1% ,86.8%,80.9% and 61.2% respectively (30).

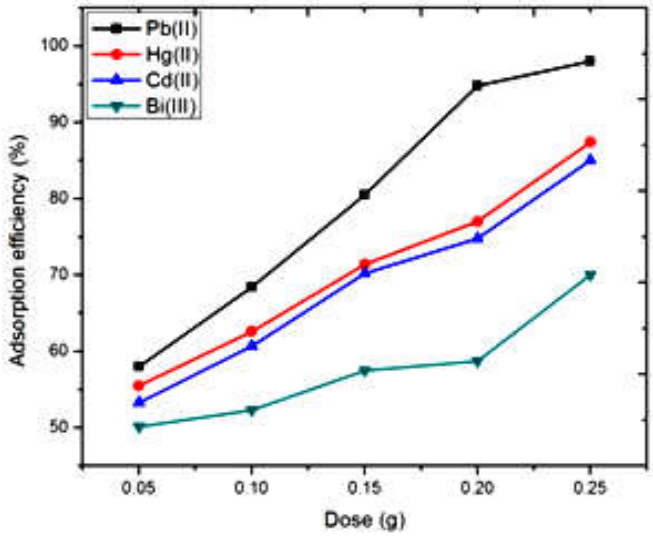

Figure.12.Effect of adsorbent dosage on percentage removal of Pb(II), Hg(II), Cd(II) and Bi(III) onto n-ZPFR

Adsorption isotherms

Adsorption isotherms is the most important design can be used to explained the interactions between adsorbents and adsorbates, as well as the adsorption capacity of adsorbents. The adsorption isotherm shows how the adsorbate molecules are distributed between the liquid phase and solid phase. The analysis of the isotherm data by fitting them to different isotherm model is an important step to find the suitable model that can be used for design purposes. The correlation of equilibrium data is essential for practical design and operation of adsorption systems.

The Langmuir isotherm which has been successfully applied to many sorption processes can be used to explain the sorption of metal ions. Langmuir model (31) assumes that the uptake of Pb (II), Hg(II), Cd(II) and Bi(III) ions occurs on a homogeneous surface by monolayer adsorption without any interaction between adsorbed ions. Isotherms are the equilibrium relations between the concentration of adsorbate on the solid phase and its concentration in the liquid phase. From the isotherms the maximum adsorption capacity can be obtained. These data provide information on the capacity of the sorbent or the amount required to remove a unit mass of pollutant under the system conditions. Data has been subjected to different adsorption isotherms. The Langmuir (32) parameters can be used to predict affinity between the adsorbate and the adsorbent using the dimensionless constant separation factor (R_L), given by equation

$$R_L = 1/1+bC_0 \quad \text{..... (4)}$$

Where R_L is the dimensionless separation factor,C_0 is the initial concentration of the adsorbate (mg L^{-1}),and b is the Langmuir constant (L mg^{-1}) .

The R_L can be used to verify that the adsorption in the system studied is unfavorable (R_L less than 1), linear (R_L=1). Favorable (0 less than R_L less than 1),or irreversible (R_L=0).The value of R_L decreased with an increase in the initial concentration, says that the adsorption is more favorable at high concentration shows the equilibrium isotherms data as points for the adsorption of Pb(II), Hg(II), Cd(II) and Bi(III) ions by ZnO nanoparticles. These isotherm data have been analyzed for the Langmuir and Freundlich isotherms by linear method of analysis.

The linear form of Langmuir isotherm is given by:

$$C_e/q_e = 1/K_L \times q_m + C_e/q_m \quad \text{..... (5)}$$

Where, q_m is the maximum adsorption capacity, K_L is the Langmuir bonding energy coefficient. The K_L and q_m can be calculated from the intercept and slope of the linear plot of C_e/q_e against C_e shown in (Fig.13).

The Freundlich model is the earliest known empirical equation and is shown to be consistent with exponential distribution of active centers, characteristic of heterogeneous surfaces. The linear form as follows:

$$\log qe = \log KF + 1/n \log Ce \quad \text{..... (6)}$$

Where, 'K_F ' and 'n' are the Freundlich isotherm constants indicating the adsorption capacity and adsorption intensity,(33,34) respectively. The K_F and n can be calculated from the intercept and slope of the linear plot of log qe against log Ce. The value of n >1 is favorable and heterogeneous adsorption for all metal ions (35). All the metals did not follow the Freundlich isotherm as closely as the Langmuir isotherm. Temkin isotherm models assume that the heat of adsorption for all the molecules in the layer decreases linearly with coverage due to adsorbent-adsorbate interactions. The data were analyzed according tothe linear form of the Temkin model.

$$q_e = B_1 \ln K_T + B_1 \ln C_e \quad \text{..... (7)}$$

The isotherm constants B_1 and K_T are related to the maximum binding energy and heat of adsorption. The $B_1$and K_T can be calculated from the intercept and slope of the linear plot of qe against ln Ce. The Freundlich and Langmuir isotherm models could not elucidate clearly the type of biosorption behavior (physical or chemical).

Dubinin-Kaganer- Radushkevich (DKR) isotherm model DKR model (36,37) is significant for calculating the apparent energy of adsorption, which predicts the type of adsorption i.e. physisorption or chemisorption. The model can be represented as (Dubinin and Radushkevich, 1947) :

$$\ln q_e = \ln q_m - \beta\varepsilon^2 \quad \text{..... (8)}$$

Where, β a constant related to the adsorption energy (mol2/kJ2), qm is a constant that indicates the sorption degree characterizing the sorbent (mg/g) and ε is the Polanyi potential shown in Eq.8:

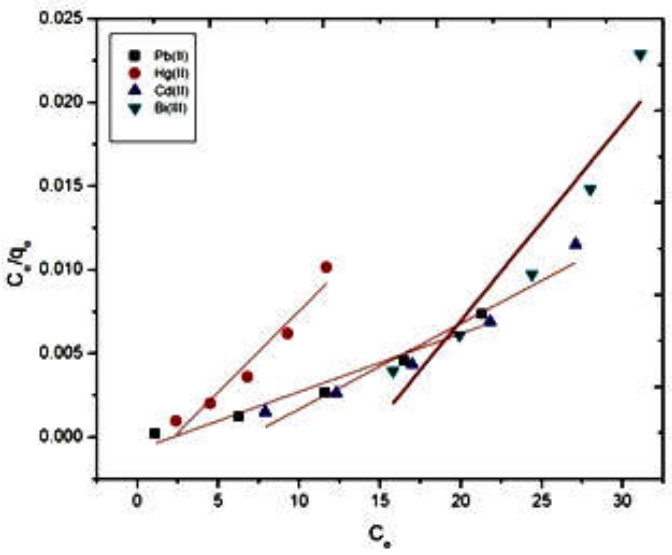

Figure 13. Langmuir isotherm plots for the adsorption of Pb (II), Hg (II), Cd (II) and Bi (III) onto n-ZPFR

$$\varepsilon = RT \ln (1+1/Ce) \quad \text{..... (9)}$$

where $\varepsilon = RT \ln (1+1/C_e)$ is polanyi potential. The plot of ln q_e vs ε^2 yielded a straight line, thereby confirming the applicability of the model (Fig.14). The value of β was calculated from the slope of the plot which was used to calculate the adsorption energy, E (= $1/(2\beta)^{1/2}$).

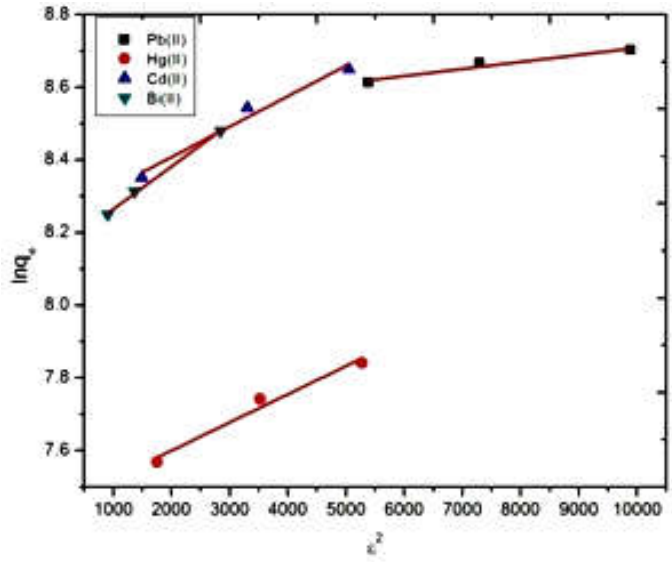

Figure 14. DKR adsorption isotherm models for adsorption of Pb (II), Hg (II), Cd (II) and Bi (III) onto n-ZPFR composite

The biosorption type based on the D-R model can be expressed by the mean free energy (kJ/mol) employing Eq.10:

$$E = 1/ (2\beta) ½ \quad \text{..... (10)}$$

E values are useful in estimating the type of adsorption. The mean free energy of adsorption for the present study was found to be energy values for the adsorption of Pb(II), Hg(II), Cd(II), and Bi(III) in the range 0.08002 KJ/mol to 0.42697 KJ/mol indicate a physical adsorption.

Table 1. Different adsorption isotherm model parameters for the adsorption of Pb(II), Hg(II), Cd(II) and Bi(III) on n-ZPFR

Mathematical Models	Parameters	Pb(II)	Hg(II)	Cd(II)	Bi(III)
Langmuir isotherm	R^2	0.955	0.949	0.944	0.91
	K_L	3.4772	9.7033	5.1228	0.00118
	q_m(mg/g)	0.2875	0.1030	0.1952	847.457
Freundlich isotherm	R^2	0.786	0.889	0.916	0.941
	K_F	6362	2172	9772	3.9810
	N	4.6511	2.1231	1.5649	0.6540
Temkin isotherm	R^2	0.860	0.946	0.969	0.991
	B_1	963.1	851.61	2401	3849.7
	K_T	6393.3	3389.6	1051.6	1470.1
D-R isotherm	R^2	0.915	0.952	0.953	0.996
	B	1.93813E-5	7.76598E-5	8.38598E-5	1.17103E-4
	q_m(mg/g)	4988.7	1710.2	3790.6	3455.7
	E k_J/mol	2579.8	643.8	596.2	426.9
Jovanoic isotherm	R^2	0.989	0.986	0.986	0.977
	K_J(L/mg)	0.035	0.084	0.042	0.069
	q_m(mg/g)	8.768	8.074	8.957	9.438

Table 2. Kinetics parameters for the adsorption of Pb(II), Hg(II), Cd(II) and Bi(III) on n-ZPFR

Mathematical models	Parameters	Pb(II)	Hg(II)	Cd(II)	Bi(III)
First-order kinetics	R^2	0.963	0.849	0.969	0.968
	K_1 (min^{-1})	5.2874	0.00251	0.00291	0.00672
	q_e (mg/g)	144.82	109.95	135.8	120.69
Second-order kinetics	R^2	0.999	0.998	0.995	0.987
	K_2 g/mg/min	0.1682	3519.51	0.31295	1254.85
	q_e(mg/g)	0.6156	0.2706	0.5775	0.5012
Intra-particle diffusion	R^2	0.993	0.976	0.941	0.936
	K_{id} g/mg/$min^{1/2}$	0.021	0.012	0.005	0.003
	C (mg/g)	124.03	25.44	22.61	6.99

The Jovanoic isotherm (Jovanoic, 1969), which is based on the same assumptions of the Langmuir isotherm, also considers the possibility of some mechanical contacts between the adsorbing and desorbing molecules on the homogeneous surface and can be represented in a linear form as follows:

$$\mathbf{\ln q_e = \ln q_m + KJ\ Ce} \quad \ldots\ldots\ldots\ldots\ldots \mathbf{(11)}$$

Where, $q_m$is the maximum amount adsorbed (in mg/g) and KJ (in L/mg) is the constant related to the energy of adsorption. The qm and KJ can be calculated from the intercept and slope of the linear plot of ln qe against Ce (Fig.15). To understand the adsorption equilibrium behavior, five isotherms, namely Langmuir, Freundlich, Temkin, D-R and Jovanoic isotherm models were tested and the Table 1 summarized the isotherm parameter values. The best fitted models were selected on the basis of coefficient Jovanoic isotherm and D-R isotherm model. The Jovanoic isotherms were best fit model for the adsorption of Pb(II), Hg(II), Cd(II) and Bi(III) onto n-ZPFR.

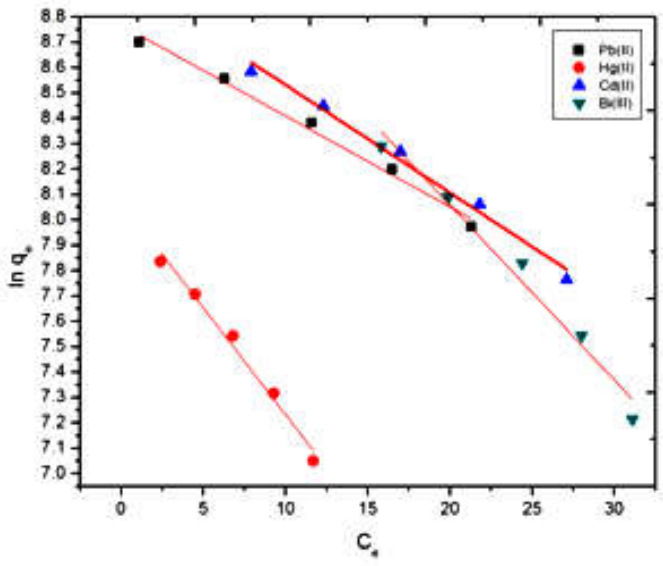

Figure 15. Jovanoic Isotherm plots for the adsorption of Pb (II), Hg (II), Cd (II) and Bi (III) onto n-ZPFR

Kinetic modeling

In order to explain the mechanism and to determine the rate controlling step of adsorption for Pb(II), Hg(II), Cd(II) and Bi(III) onto n-ZPFR, kinetic models were used. The rate constants were calculated by using pseudo-first-order and pseudo-second-order kinetic models and the rate controlling step was described by intra-particle diffusion model and the Table 2 summarized the kinetic parameter values.

Pseudo-first-order model

The pseudo-first-order kinetic model (Lagergren, 1898; Smiciklas *et al*., 2008) has been widely used to predict sorption kinetics. The equation of the model was represented as follows:

$$\mathbf{\ln(q_e - q_t) = \ln q_e - k_1 t} \quad \ldots\ldots\ldots\ldots\ldots \mathbf{(12)}$$

where q_e is the amount of metal ions adsorbed per unit weight of adsorbent at equilibrium ie; adsorption capacity (mg/g) ,q is the amount of adsorbent adsorbed (mg/g) at any time t and k_1 is the rate constant. The value of k_1 was calculated from the slope of the linear plot of ln (q_e-q_t) versus t.

Pseudo-second-order rate model

The linear form of pseudo-order kinetic model (41) was expressed by equation

$$t/q_t = 1/k_2 \times q_e^2 + t/q_e \quad \text{..... (13)}$$

Where k_2 (g/mg/min) is the second-order rate constant of adsorption. The plot of t/q_t versus t shows a linear form. The equilibrium adsorption capacity q_e and the values of k_2 were calculated from the intercept and slope of the plot represented in (Fig.16)

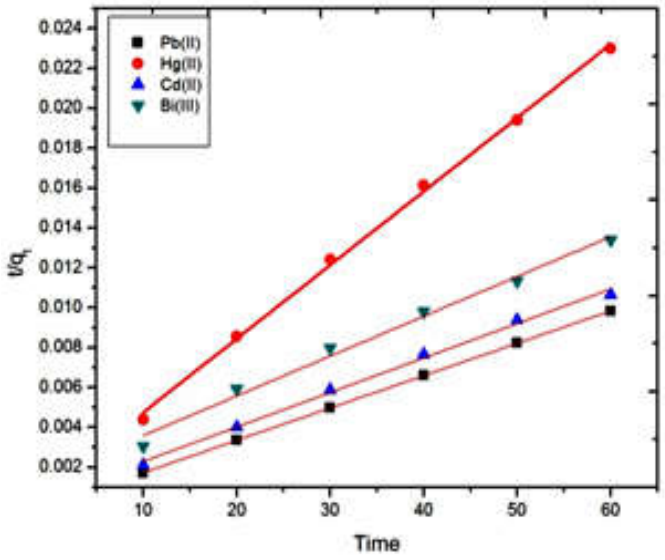

Figure 16. Pseudo-second order kinetic plots for adsorption of Pb (II), Hg (II), Cd (II) and Bi (III) onto n-ZPFR

Intra-particle diffusion model

The overall reaction kinetics for the adsorption of Pb(II), Hg(II), Cd(II) and Bi(III) is a pseudo-second order process. However this could not highlight on the rate-limiting step.The rate-limiting step (slowest step of the reaction) may be either the boundary layer (film) or the intra-particle (pore) diffusion of solute on the solid surface from bulk of the solution in a batch process (Fig.17). The intra-particle diffusion model proposed by Weber and Morris (Weber and Morris, 1964; Weber and Morrism, 1964; Weber and Morris, 1963; Sairam Sundaram *et al*., 2008) was used to identify the mechanism involved in the adsorption process:

$$q_t = k_{id} t^{0.5} + c \quad \text{..... (14)}$$

where q_t is adsorption capacity at any time t and k_{id} is the intra-particle diffusion rate constant (mg g^{-1} $min^{-0.5}$) and C (mg/g) reflects the boundary layer effect. Greater the value of C greater is the effect of boundary layer on adsorption process. If the rate limiting step be the intra-particle diffusion, the plot of q_t against the square root of time should be a straight line and pass through the origin. The deviation of the plot from the linearity indicates the rate-limiting step should be boundary layer (film) diffusion controlled.

The k_{id} and C can be determined from the slope and intercept of the linear plot of q_t against $t^{0.5}$The pseudo-first order. pseudo-second order and intra-particle diffusion models were used to understand the kinetic nature of Pb(II), Hg(II), Cd(II) and Bi(III) onto n-ZPFR adsorption system. All the experimental data showed better agreement with pseudo-second order model in terms of higher correlation coefficient value (R^2>1), which suggested the adsorption rate of Pb(II), Hg(II), Cd(II) and Bi(III) onto n-ZPFR might be controlled by chemisorptions mechanism. The rate controlling step consisted valence forces through sharing or exchange of electrons between the adsorbent surface and adsorbate ions and no involvement of mass transfer in solution (46). The value of pseudo-second-order rate constant ,k_2,was 0.168 g/mg/min for Pb(II), 3519.51 g/mg/min for Hg(II), 0.31295g/mg/min for Cd(II) and 1254.85g/mg/min for Bi(III).

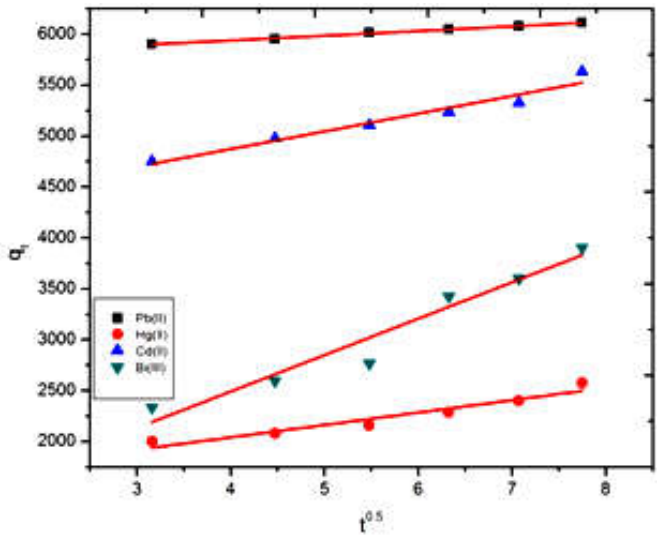

Figure 17. Intra-particle diffusion

Effect of temperature and Thermodynamics Data

The adsorption of metal ions were studied at three different temperatures at 308k,318k and 328k,respectively.For kinetic studies, a series of 250ml flask were used and each flask was filled with n-ZPFR at mass loadings 0.250g for all the metal ions solution at 0.01M.The percentage removal of all the metal ions are shown in (Fig.18).

This indicates that the adsorption of metal ions on n-ZPFR is endothermic in nature. The increase in the rate of adsorption with the increase in temperature may be attributed to the strong adsorptive forces between the active sites of the adsorbents and adsorbate species and also between the adjacent molecules of the adsorbed phases. Thermodynamic parameters, such as change in enthalpy (ΔH^0), change in entropy (ΔS^0) and change in free energy (ΔG^0),were determined using the following equations (Biswas *et al*., 2007; Ahmet Sari *et al*., 2007).

$$K_L = q_e/c_e \quad \text{..... (15)}$$

Where K_L is the Langmuir constants; C_e is the concentration of solute adsorbed on the resin at equilibrium, mg/L.

$$\Delta G^0 = -RT\ln K_L \quad \text{..... (16)}$$

The ΔH^0 and ΔS^0 were obtained from the slope and intercept of van't Hoff plot of ln K_L versus 1/T plot shown in (Fig.19), according to the following equation:

$$\ln K_L = \Delta S^0/R - \Delta H^0/RT \quad \text{..... (17)}$$

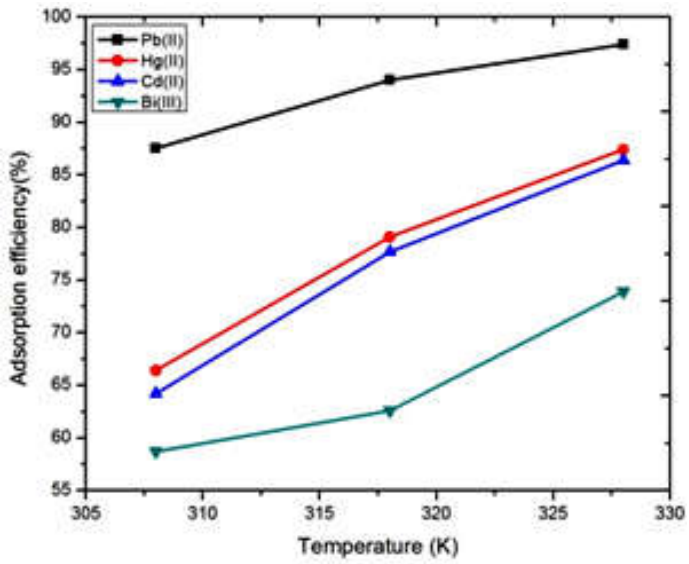

Figure 18. Effect of Temperature

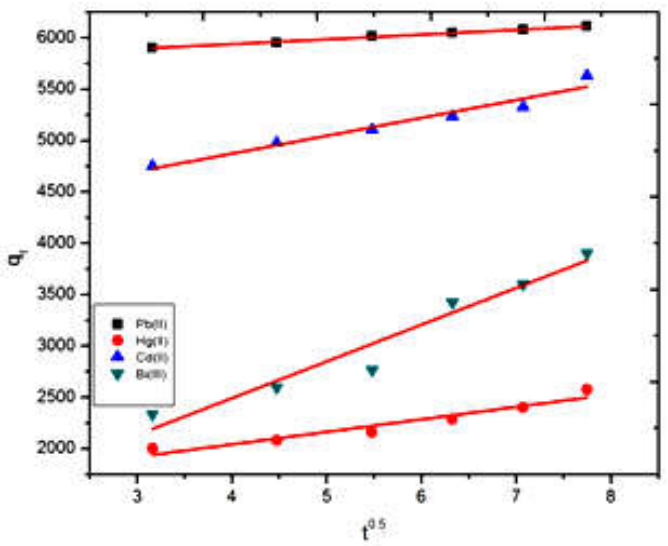

Figure 19. van't Hoff plots of $\ln K_L$ versus 1/T for the adsorption of Pb (II),Hg (II), Cd (II)and Bi (III)

Where, R is the gas constant (8.314 J/mol K),T is the temperature in Kelvin. The values of these parameters thus calculated are recorded in Table 3.The correlation coefficient for the linear plot for Pb(II), Hg(II), Cd(II) and Bi(III) was R^2=0.999, R^2 =0.999, R^2 =0.999 and R^2 =0.812.The positive values of standard enthalpy change (ΔH^0) for the intervals of temperatures showed the endothermic in nature of the adsorption process. The low enthalpy values of ΔH^0 less than 20kJ/mol indicates that the physisorption is involved in the process of adsorption. The positive value of entropy change ΔS^0 corresponds to a increase in degree of freedom of the adsorbed species and thereby increase in concentration of adsorbate in solid-solution interface which takes place through ion exchange interactions (Malkoc and Nuhoglu, 2007).

The negative values of ΔG^0 at all temperatures indicated the spontaneous nature of the adsorption of Pb(II), Hg(II), Cd(II) and Bi(III).It indicated that the adsorption efficiency of all metal ions onto ZnO nanoparticles increases with increases in temperature, this trend to be assigned to the dissolution of ZnO nanoparticles at higher temperatures (Mustafa *et al*., 2002). The negative values of ΔG^0 confirm the feasibility of the process at all temperatures and the spontaneous nature of adsorption with a high preference for Pb(II) compared to Hg(II),Cd(II) and Bi(III) onto n- ZPFR.

Table 3. Thermodynamic parameters for the adsorption of Pb(II), Hg(II), Cd(II) and Bi(III) onto n-ZPFR

Metal ions	R^2	ΔH^0	ΔS^0	$-\Delta G^0$ (KJ/mol)		
				308K	318K	328K
Pb(II)	0.999	42.33	197.13	-65.88	-81.90	-97.65
Hg(II)	0.999	52.42	218.11	-29.57	-47.64	-65.53
Cd(II)	0.999	53.33	220.22	-26.95	-45.46	-63.32
Bi(III)	0.812	28.85	138.29	-21.06	-26.10	-41.27

Desorption Studies

Desorption studies of the adsorbed metal ions from n-ZPFR composites was carried out by HCl solution at room temperature. Desorption percentage was calculated as follow;

$$\text{Desorption (\%)} = C_e^{\,1}\, V/q_m \times 100\ \% \qquad \text{..... (18)}$$

Where q is the adsorption capacity (mg/g), m is the mass of the adsorbent (mg), V is the volume of the aqueous solution (ml), $C_e^{\,1}$ is the concentration of metal ions aqueous solution after desorbed from the adsorbent. For regeneration, the adsorbent was removed from the solution and rinsed with DD water. The adsorption–desorption cycles were repeated for 5 times, and desorption percentage was calculated. The results showed that the elution ratio is different under various eluent concentrations. Maximum recovery of Pb (II), Hg(II), Cd(II) and Bi(III) at 100%, was achieved with 2 and 3M HCl eluent solutions, respectively. Recovery and recyclability of adsorbents in aqueous reaction system are regarded as a crucial property in the purification systems of wastewater.

Conclusion

The main objectives of this paper are to identify the various parameters that affect the adsorption, such as adsorbent dose, initial concentration, contact time, temperature and P^H .To analyze the equilibrium uptake capacity of the adsorption process from various adsorption isotherms models like D-R, Jovanoic isotherm equation. Present study reported the mechanism of adsorption of Pb (II), Hg(II), Cd(II) and Bi(III) onto nano ZPFR prepared via polymerization method. The D-R and Jovanoic model provided the best fit for the Pb(II), Hg (II) ion, Cd(II) and Bi(III) revealing the maximum adsorption capacity of Pb(II) 8.768 mg/g and Hg(II) 8.074 mg/g respectively.

The lower values of R_L and n < 1 indicated that the adsorption process was favored for nano ZPFR. Kinetic studies demonstrated that the mechanism for adsorption of metal ions followed the pseudo-second order rate model, which provided the best fit for all the metal ions. The thermodynamic studies revealed that the adsorption is spontaneous and endothermic in nature for Pb (II), Hg(II), Cd(II) and Bi(III) ions onto nano ZPFR. The positive entropy indicated increase in the degree of freedom for the adsorbed species and suggests that there is an increase in the concentration of adsorbate in solid-liquid interface.

Acknowledgement

The authors wish to acknowledge the management and Department of Chemistry, Thiagarajar College, Madurai-9, for providing lab facilities.

REFERENCES

Ahmet Sari, Mustafa Tuzen , Demirhan Citak, Mustafa Soylak 2007. Equilibrium, Kinetics and thermodynamic studies of adsorption of Pb(II) from aqueous solution onto Turkish Kaolinite clay, *Journal of Hazardous Materials,* 149:283-291.

Barakat, M.A. 2011. New trends in removing heavy metals from industrial wastewater. *Arabian Journal of Chemistry,* 4: 361-377.

Biswas, K., Saha, S.K. and Ghosh, V.C. 2007. Adsorption of fluoride from aqueous solution by a synthetic iron (III) aluminum(III) mixed oxide. *Ind. Eng. Chem. Res.,* 46: 5346- 5356.

Bonner, O., Easterling, G., Weit, D. and Holland, V. 1955. Osmotic and activity coefficients of P-toluene sulfonic acid and p-ethyl benzene sulfonic acid and their relationship to ion exchange equilibria, *J. Am. chem. Soc.,* 77:242-244.

Chang, B.S., Zhang, X.R., Guo, J., Sun, Y, Tang. H.Y., Ren. Q.G. and Yang, W.L. 2012. General one-pot strategy to prepare multifunctional nanocomposites with hydrophilic colloidal nanoparticles core/mesoporous silica shell structure, *J. Colloid Inter-face Sci.,* 377:64-75.

Cheng, K., Zhou, Y.M., Sun, Z.Y., Hu, H.B., Zhong, H., Kong. X.K. and Chen, Q.W. 2012. Synthesis of carbon-coated, porous and water-dispersive Fe_3O_4 nanocapsules and their excellent performance for heavy metal removal applications, Dalton Trans., 41:5854-5861.

Denizli, A., Senal, S., Alsancak, G., Tuzmen, N. and Say, R. 2003. Mercury removal from sunthetic solutions using poly (2-hydroxyethylmethacrylate) gel beads modified with Poly (ethyleneamine). Reactive and Functional polymers 55: 121-130.

Dlarmendra, K. Tiwari, Behari, J. and Prasenjit Sen, 2008. Application of nanomaterials in wastewater treatment. *World Applications science Journal*, 3: 417-433.

Dubinin, M. and Radushkevich, M.L.V. 1947. The equation of the characteristic curve of activated charcoal. Dokl. Akad. Nauk SSSR 55:327-329.

Febrianto, J., Kosasih, A.N., Sunarso, J., Ju, Y.H., Indraswati, N., *et al*. 2009. Equilibrium and kinetic studies in adsorption of heavy metals using biosorbent: a summary of recent studies. *J. Hazard Mater,* 162: 616-645.

Foo, K.Y. and Hameed, B.H. 2010. Insights into the modeling of adsorption isotherm systems. *J. Chem. Eng.,* 156: 2-10.

Fujita, M., lde, Y., Sato, D. *et al*. 2014. Heavy metal contamination of coastal lagoon sediments. Fongafale islet, Funafuti atoll, tuvalu, *Chemosphere*, 95: 628–634.

Hall, K.R., Eagleton, L.C., Acrivos, A. and Vermevlen, T. 1966. Pore and Solid diffusion kinetics in fixed bed adsorption under constant pattern conditions. *Indian Engineering and chemistry Fundamentals,* 5: 212-219.

Ho, Y.S., Mckay G. Wase, and Forster, C.F. 1963. Study of the adsorption of divalent metal ions onto peat, Adsorption *science and Technology Am Soc Civ Eng.,* 89: 31-60.

Inglezakis, V.J., Loizidou, M.D. and Grigoropoulou, H.P. 2003. Ion exchange of $Pb^{(2+)}$ $Cu^{(2+)}$ $Fe^{(3+)}$ and $Cr^{(3+)}$ on natural clinoptilolite: selectivity determination and influence of acidity on metal uptake. *J. Colloid Interface Sci.,* 261: 49-54.

Jing Hu, M.C. Irene and Guohua Chen, 2005. Fast removal and recovery of Cr (VI) using surface- modified jacobsite ($MnFe_2O_4$) nanoparticles, Langmuir, 21:11173-11179.

Jing-Fu Liu, Zond-Shan Zhao, Gui-Bin Jiang and Coating 2007. Fe_2O_4 magnetic nanoparticles with humic acid for high efficient removal of heavy metals in water, *Environmental science and Technology,* 42:6949-6954.

Jovanoic, D.S. 1969. Physical adsorption of gases I. Colloid and Polymer science 235l: 1203-1214.

Kannan, N. and Seenivasan, R.K. 2007. Synthesis and studies of phenol-formaldehyde cationic exchangers blended with sulphonated Eugenia jambolana, lam, Carbon, Desaline, com, 216:77-87.

Kannan, N., Mukunthan, K.S. and Balaji, S. 2011. A comparative study of morphology, reactivity and stability of synthesized silver nanoparticles using bacillus subtilis and catharanthus roseus (L.) G. Don. colloids surf B 86:378-383.

Kawasaki, N., Bun-el, R., Ogata, F., Nakamura, T., Tanei, S., *et al*. 2006. Water treatment technology using carbonaceous materials produced from vegetable biomass, *Journal of water and Environmental Technology,* 4: 73-82.

Lagergren, S. 1898. About the theory of so-called adsorption of soluble substance, K. Svenska Vetenskapsakad Handl 24: 1-39.

Langmuir, I. 1918. The adsorption of gases on plane surfaces of glass, mica and platinum, *Journal of American chemical society,* 40: 1361-1403.

Liu, J.W., Cheng, J., Che, R.C., Xu, J.J., Liu, M.M. and Liu, Z.W. 2013. Double-shelled yolk-shell microspheres with Fe_3O_4 cores and SnO_2 double shells as high –performance microwave adsorbers, *J. Phys. Chem.,* C 117, 489-495.

Malkoc, E. and Nuhoglu, Y. 2007. Determination of kinetic and equilibrium parameter of the batch adsorption of *Quercus itnaburensis. Chemical Engineering Process,* 46: 1020-1029.

Mckay, Y.S.G. 1999. Pseudo-second order model for sorption processes. *Proc. Biochem.* 34:451-465.

Mohamed Abdel Salam and Robert C. Burk, 2010. Thermodynamics and kinetics studies of pentachlorophenol adsorption from aqueous solutions by multi-walled carbon nanotubes, water, air, and soil pollution 210:101-111.

Mustafa, S., Shahida, P. Naeem, A. Dilara, B. and Rehana, N. 2002. Sorption studies of divalent metal ions on ZnO. Langmuir 18:2254-2259.

Nata, I.F., Salim, G.W. and Lee, C.K. 2010. Facile Preparation of magnetic carbonaceous nanoparticles for Pb^{2+} ions removal*, J. Hazard. Mater,* 183:853-858.

Ngah, W.S.W., Endud, C.S. and Mayanar, R. 2002. Removal of copper (II) ions from aqueous solution onto chitosan and cross-linked Chitosan beads. *React Funct Polym.,* 50: 181-190.

Oh, H.D. Kim, S.O. Lee, J.K. and Lee, S.W. 2013. Facile synthesis of carbon layer-entangled Fe_3O_4 clusters as anode materials for improved Li-ion batteries*, J. Power sources,* 244 (2013) 575-580.

Ozsoy, H.D., Kumbur, H., Saha, B. and Leeuwen, J.H.W. 2008. Rhizopus oligosporus produced from food processing wastewater as a biorsorbent for cu(II) ions

removal from the aqueous solutions, *Journal of Bioresource Technology,* 99:4943-4948.

Rahmani, A., Zavvar, H., Mousavi, M. and Fazli, 2010. Effect of nanostructure alumina on adsorption of heavy metals, Desalination 253:94-100.

Sairam Sundaram, C., Natrayasamy Viswanathan and Meenakshi, S. 2008. Deflorination chemistry of synthetic hydroxyapatite at nano scale: equilibrium and kinetic studies, *Journal of Hazardous Materials,* 155:206-215.

Sankar, R., Karthick, A., Prabu. A, Karthick. S, Subramanian. K. and Ravikumar, V. 2013. Origanum vulgare mediated biosynthesis of silver nanoparticles for its antibacterial and anticancer activity, colloids surf B, 108:80-84.

Schwarzenbach, R.P., Egli, T., Hofstetter, T.B., Von Gunten, U. and Wehrli, B. *et al*. 2010. Global water pollution and human health. *Annual Review of Environment and Resources*, 35: 109–136.

Senthilnathan J. Ligy Philip, 2010. Removal of mixed pesticides from drinking water system using surfactant assisted Nano-TiO_2 , water, Air, and soil pollution, 210:143-154.

Smiciklas, I., Onjia, A., Raicevic, S., Janackovic, D., Metric, M. 2008. Factors influencing the removal of divalent cations by hydroxyapatite, *Journal of Hazardous Materials,* 152:876-884.

Smiciklas, L., Onjia, A., Raicevic, S., Janackovic, D. and Metric, M. 2008. Factors influencing the removal of divalent cations by hydroxyapatite, *J. Hazard. Mater,* 152: 876-884.-

Srivastava, S.K., Bhattacharjee, G., Tyagi, R., Pant, N. and Paul, N. 1988. Studies on the removal of some toxic metal ions from aqueous solutions and industrial waste, Part I (Removal of lead and cadmiumby hydrous ion and aluminium oxide), *Environ Technol Lett.,* 9:1173-1185.

Thongnopkun, P., Jamkratoke, M. and Ekgasit, S. 2012. Thermal behavior of nanosilver clay in the application of handmade jewelry, *Mater. Sci. Eng.,* 556:849-854.

Weber, Jr W.J., Morris, J.C. 1963. Kinetic of adsorption on carbon from solution. *J. Sanit Eng Div Am Soc Civ Eng.,* 89: 31-60.

Weber, W.J. and Morris, J.C. 1964. Equilibria and capacities for adsorption on carbon, *Journal of the sanitary Engineering Division,* 90:79-107.

Weber, W.J., Morris, 1964. Advances in water pollution research. Pergamon Press. Oxford.

Xiaowang Liu, Oiyan Hu, Zhen fang, Xiaojur, Zhang and Beibei Zhang, 2009. Magnetic chitosan nanocomposites: a useful recyclable tool for heavy metal ion removal, Langmuir, 25:3-8.

Xue-Song Wang, Juan Huang, Huai-Qiong Hu, JingWang,Yong Qin, 2007. Determination of Kinetic and equilibrium parameters of the batch adsorption of Ni(II) from aqueous solution by Na-mordenite, Journal of Hazardous Materials 142:468-476.

Zagorodni, A.A. Kotova, D.L. and Selemenev, V.F. 2002. Infrared spectroscopy of ion exchange resins; chemical deterioration of resins, *Reac. Func, Poly.,* 53:157-171.

Zhang, X.F., Wang, J., Li. R.M, Dai. Q.H, Gao. R, Liu. Q, Zhang. M.L. 2013. Preparation of Fe_3O_4@Layered double hydroxide composite for magnetic separation of uranium, *Ind. Eng. Chem. Res.,* 52:10152-10159.

Zhang, Y.F., Liu, X.H., Nie, J.R., Yu, L., Zhong, Y.L. and Huang, C. 2011. Improve the catalytic activity of α-Fe_2O_3 particles in decomposition of ammonium perchlorate by coating amorphous carbon on their surface, *J. Solid state chem.,* 184:387-390.

Zhao, G.H., Wang, J.Z. Li, Y.F., Chen, X. and Liu, Y.P. 2011. Enzymes immobilized on super paramagnetic Fe_3O_4@Clays nanocomposites: preparation, characterization, and a new strategy for the regeneration of supports, *J. Phys. Chem.,* C 115:6350-6359.

****